Resources, Conservation & Recycling 223 (2025) 108500

Contents lists available at ScienceDirect

Resources, Conservation & Recycling

journal homepage: www.sciencedirect.com/journal/resources-conservation-and-recycling

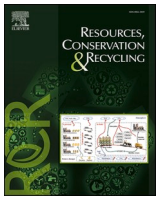

Alloy selective optical sorting of mixed post-consumer aluminum scrap streams

Mert Efe [a,*], Aashish Rohatgi [a], Qiang Dai [b], Brian Stapleton [b], Kate Rader [a], Albert L. Lipson [b], Jeffrey S. Spangenberger [b]

[a] Pacific Northwest National Laboratory, Richland, WA, 99354, USA
[b] Argonne National Laboratory, Lemont, IL, 60439, USA

ARTICLE INFO

Keywords:
Aluminum
Recycling
Optical sorting
Surface coating
Wrought
Twitch
Domestic resources

ABSTRACT

Shredded post-consumer aluminum scrap streams contain a mixture of cast and wrought aluminum pieces with very different compositions, resulting in downcycling of the mixed scrap into non-structural cast aluminum alloys and parts. In this paper, we introduce a chemical treatment method to color-code scrap aluminum pieces by alloy family and demonstrate low-cost optical sorting of cast from wrought pieces to upgrade the scrap stream. The color difference enabled > 95 % purity in the optically sorted cast and wrought fractions. We also colored wrought aluminum pieces and scrap by alloy families, such as 5xxx and 6xxx, which has the potential to create a circular supply chain in which wrought aluminum alloys are sorted from the mixed scrap stream and recycled back to high-value wrought products. Our TEA and LCA show feasibility of our coloring method and optical sorting, and we discuss the implications for the U.S. aluminum and transportation industries.

1. Introduction

As manufacturing sectors in U.S. and other countries work towards increasing their production capacities while utilizing more domestic resources, innovations around more efficient use of raw materials and recycling are necessary (Van den Eynde et al., 2022). Aluminum (Al) with abundant scrap resources is widely used in multiple manufacturing industries. Several studies are predicting an incoming wave of scrap surplus mainly from aluminum used in transportation applications (Van den Eynde et al., 2022; Zhu et al., 2021). A key to address the scrap surplus and utilize domestic aluminum scrap resources is to develop more economical means of recycling aluminum and in a way that does not degrade its value or properties (Van den Eynde et al., 2022; Løvik et al., 2014). A good example to efficient recycling is beverage cans, which are nearly entirely made from recycled Al. Such complete utilization of recycled Al in beverage cans is possible because the cans are roughly identical in shape and size, pre-sorted at the point of collection, and comprise standardized wrought Al alloys (5xxx Al for the can end and 3xxx Al for the can body) (Schlesinger, 2013). However, recycled aluminum use in transportation (automotive), building and construction, and consumer durables applications is more challenging and complex due to a mix of cast and wrought (sheets, extrusions, forgings) parts with very different (and incompatible) chemistries and forms (Schlesinger, 2013; Das et al., 2010). As a result, cast aluminum parts contain about 60 % scrap, and wrought parts contain only about 25 % scrap (Raabe et al., 2022).

Shredded post-consumer scrap streams of aluminum such as Zorba and Twitch contain 6 major alloy families shown in Fig. 1. The low recycled content in wrought products arises from the mixed recycling of cast and wrought alloys and therefore a high content of Si in the scrap along with other alloying elements (Zhu et al., 2025). For instance, a typical cast alloy (e.g. 356 Al) contains a total of 9 wt. % alloying elements including 7 % Si by weight, whereas a typical sheet alloy (e.g. Al 6111) contains 3 wt. % alloying elements with maximum 1.1 % Si by weight. In particular, Si and Fe must be limited in wrought alloys to maintain their mechanical properties (Raabe et al., 2022; Das et al., 2007). The shredded scrap therefore is mostly downcycled to lower value cast products with wider composition ranges. A cost-effective sorting method of the cast and wrought material from the mixed stream into individual alloy families can enable recycling of wrought scrap back into the wrought products at a much higher recycled percentage (Løvik et al., 2014; Zhu et al., 2025; Kelly and Apelian, 2017).

There are several methods to sort mixed shredded aluminum scrap, each with its own advantages and disadvantages:

* Corresponding author at: Energy and Environment Directorate, Pacific Northwest National Laboratory, 902 Battelle Blvd., Richland WA 99354, USA.
E-mail address: mert.efe@pnnl.gov (M. Efe).

https://doi.org/10.1016/j.resconrec.2025.108500
Received 1 April 2025; Received in revised form 29 June 2025; Accepted 7 July 2025
Available online 11 July 2025

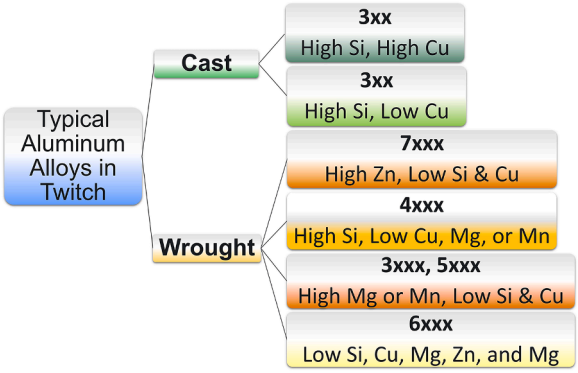

Fig. 1. Typical cast and wrought alloys found in the Twitch stream.

(a) Laser induced breakdown spectroscopy (LIBS) and (b) x-ray fluorescence (XRF) are spectroscopy-based, which makes them highly precise in detecting alloy composition and can successfully separate cast from wrought scrap, as well as further sort by individual alloy (Schlesinger, 2013). The throughput of these systems is between 3 and 8 tons/hr, which is slower than other sensor-based sorting methods or physical separation methods based on density and shape (Schlesinger, 2013; Díaz-Romero et al., 2021). Due to low penetration depth of x-rays in metals, the surface of the scrap needs to be completely clean or else paints/dust/oil etc. can lead to incorrect or no identification at all (Brooks and Gaustad, 2021).

(b) X-ray transmission (XRT) based sorters can separate cast from wrought scrap at faster rates than LIBS or XRF, up to 30 tons/hr. However, XRT is not able to identify individual alloys, and the sorted wrought scrap can still contain ~15 % cast material by weight (Kelly and Apelian, 2017).

(c) Optical sorters offer the benefits of being low cost and achieving high throughputs rates up to 150 tons/hr (Gülcan and Gülsoy, 2017). However, they require distinct visual differences in the materials to be sorted and can be sensitive to the surface condition of the scrap. Optical sorting is currently used to separate copper (reddish hue) from brass (yellow hue) due to their distinct color differences. But most shredded aluminum scrap has a very similar color irrespective of cast vs. wrought or alloy families and is therefore not amenable to color-based sorting. Recently published experiments have attempted to leverage shape differences to optically sort cast aluminum from wrought aluminum scrap, but not by individual alloy (Díaz-Romero et al., 2021; Koyanaka and Kobayashi, 2010). These techniques have successfully sorted small batches (few hundred pieces) at purities > 85 %.

(d) Hot-crush, where the scrap is preheated to temperatures above 500 °C and crushed. The cast pieces become brittle at these temperatures and can be crushed into smaller pieces while the wrought pieces remain ductile. However, this method is energy intensive and sometimes results in very small cast pieces that cannot be effectively remelted without dross losses (Ambrose et al., 1983).

(e) Magnetic induction spectroscopy leverages the conductivity differences in cast and wrought pieces. This technique can sort cast and wrought pieces at 95 % in static tests, however, sorting at commercial speeds were challenging (Williams et al., 2023).

In summary, none of the current sensor-based methods can sort shredded Al scrap by individual aluminum alloys at commercially viable production rates. In this study, we demonstrate rapid optical sorting of scrap pieces by developing color coding in aluminum alloy families based on their chemistry. To our knowledge, color-based optical sorting of aluminum alloys has not been previously reported. The most similar, publicly available work was published by Alcoa researchers in the early 2000's (Schultz and Wyss, 2000; Schultz and Wyss, 2000), where they colored well-polished coupons with solutions that left a copper contaminant residue on the specimens. However, they did not attempt to optically sort the colored pieces, nor did they demonstrated the coloring or sorting ability on realistic scrap pieces that may not develop proper color due to oxidation/dirt/paints/contaminants etc. on them. We experimented with multiple chemicals to induce color and report on their relative success. We also show the efficiencies of low-cost optical sorting in separating cast from wrought scrap pieces to upgrade the scrap stream and discuss the economic and environmental feasibility of the process. We conclude with potential implications of the sorted scrap stream for the U.S. aluminum and transportation industries.

2. Materials and methods

In this work, we studied both samples of Al with known alloy chemistries and pieces of Al scrap of unknown chemistry. Experimental coupons of known alloys were prepared from two cast alloys, A380 and A356 (representing high-Cu and low-Cu alloy families, respectively), and two sheet alloys, 6111 and 5182 (representing low-Mg and high-Mg alloy families, respectively). Supplementary Table 1 provides the compositional ranges of these alloys. These represent the most common alloy families found in the shredded post-consumer streams of Zorba and Twitch (Zhu et al., 2025). Zorba, as defined by the Institute of Scrap Recycling Industries, Inc. (recently rebranded as Recycled Materials Association, https://www.isri.org/rema), is shredded mixed non-ferrous metals consisting primarily of aluminum generated by eddy-current separator or other segregation techniques and it is the precursor of Twitch. Zorba originates from recycling of automobiles, End-of-Life Vehicles (ELVs), waste electrical, and electronic equipment, white goods (large household electrical items) and other aluminum scraps. Zorba is composed of shredded nonferrous metals such as aluminum, copper, lead, magnesium, stainless steel, nickel, tin, and zinc. To produce Twitch, Zorba is further processed usually by floatation methods using heavy media to remove all nonferrous scrap except aluminum. The Twitch scrap used in this study was provided by Alter Trading, Davenport, IA, USA. The scrap pieces were cleaned in an ultrasonic bath filled with soapy water for 5 min and later scrubbed with a wire brush to remove the dust particles and other residues left over from the wet-floatation process.

To change the surface color of the Al pieces, the samples were immersed in solutions of various chemicals, i.e. etched. Etching solutions and recipes listed in the Supplementary Table 2 were derived from the micro- and macro-etchants available in ASM handbook for Metallography and Microstructures and others (Vander Voort, 2004; Warmuzek, 2004; Vander Voort, 1999). The chemically treated pieces were then washed and dried before optical sorting. We utilized a commercial food sorter, Satake Pikasen FMS200-F full color RGB optical sorter without any modifications. It is designed to sort by size and shape of small to medium food products (mainly seeds) and plastics. Despite its compact size and 240 mm wide chute, this sorter is capable of sorting 1.8 tons/hr and is a good fit to test the rapid and low-cost sorting of shredded aluminum scrap. Larger scale belt-type optical sorters used for waste sorting, metal and mineral recycling can have belt widths up to 3 m. Belt-type sorters allow for such high throughputs due to the millisecond-fast air jets aligned along the belt width, which results in rapid ejection of pieces without overlapping. One study on mineral sorting cites optical sorting throughput as 4–5 tons/hr for the 3–5 mm fraction, increasing up to 150 tons/hr for the 100–150 mm size fraction. Their own results on magnesite sorting show throughput of up to 39 tons/hr for pieces between 25–50 mm size with purity of 86 %, assuming a sorter belt width of 3 m (Gülcan and Gülsoy, 2017). Purity depends on the throughput, and it is possible to increase purity by decreasing the throughput. Magnesite pieces used in this study ($\rho \sim 3$–3.2 g/cm^3) had very similar particle shape, color contrast, and mass as the aluminum

scrap pieces used in this study (Supplementary Table 3).

The sorted pieces were then analyzed with a Bruker S1 TITAN 600 handheld x-ray fluorescence analyzer (XRF) to confirm their chemistry and alloy type. This XRF analyzer is capable of detecting light elements like Al, Mg, Si and includes a calibration package for aluminum alloys. Some pieces were polished by sandpapers and wire brushes to improve the XRF accuracy.

The techno-economic analysis and life cycle analysis were conducted with a preliminary version of the EverLightMat model developed at Argonne National Laboratory. The model is available upon request, and key assumptions and model input are described in the supplementary file and Supplementary Tables 4 & 5.

3. Results and discussion

3.1. Color-coding of coupons of known alloys

We employed a two-step coloring process to induce color in the alloy coupons. The first step of the coloring process changes the color of the cast pieces to distinguish them from wrought pieces. Supplementary Table 2 provides the detailed results of the various chemical solutions and etching procedures that were studied for this first step. We avoided acidic solutions with hydrofluoric acidic (HF) for safety reasons, and the other non-HF acidic solutions were unsuccessful in changing color of the cast and wrought coupons. The only exception was the iron chloride ($FeCl_3$) etch, which induced different colors in each of the coupons, including the wrought alloys. Alkaline solutions, on the other, were more promising. Simple sodium hydroxide (NaOH)-water solutions gave acceptable results. The NaOH solutions with concentrations as low as 5 % etched the A356 pieces and formed a black residue on the A380 pieces without changing the appearance of the wrought pieces, which retained a dull, light grey color. The NaOH solutions generated some heat, hydrogen gas, and aluminum hydroxide ($Al(OH)_3$) deposits during etching, which could be potential hazards. Adequate cooling and ventilation of the etching environment is necessary to address the heat and hydrogen gas produced during etching. Cleaning of aluminum extrusion dies with NaOH solutions is a common practice and there is chemical processing equipment designed for this application (Tansens et al., 2011). Gluconic acid and sorbitol are commonly used to precipitate aluminum hydroxide and prevent gunk formation in NaOH solutions, significantly extending their useful life (Newman, 2018).

The second step of the coloring process changes color of the wrought alloy pieces to distinguish different alloy families. Various solutions were applied to coupons of known Al alloy to identify a suitable etching procedure for the second step. Out of all the solutions tested, ones that contained potassium permanganate ($KMnO_4$) (Weck and Leistner, 1983) and ammonium molybdate ($(NH_4)_2MoO_4$) (Beraha and Shpigler, 1977) produced the best results on the wrought alloys. The $KMnO_4$ solution produced brown and dark purple on A356 coupons; dark gray on A380; purple, blue, and green on 6111; and light gold on 5182 (Fig. 2a). The $(NH_4)_2MoO_4$ solution produced red, yellow, and blue coloring on cut surfaces of A356; no change in A380; light purple on 6111; and very light gray on 5182 (Fig. 2b). The color changes produced by other solutions were more subtle and barely visible to naked eye. For example, NaF and $K_4Fe(CN)_6$ solutions introduced some subtle hues on the sample surfaces that were only visible if the samples are tilted at certain angles.

Once suitable etching solutions were identified for each step of the coloring process, we applied the $KMnO_4$ and $(NH_4)_2MoO_4$ etchants to pieces that had been etched with NaOH solution to evaluate the effects of a two-step etch procedure. The cast pieces carried their dark brown/black color from the NaOH step, which enhanced the colors produced during the second step. Etching with the $KMnO_4$ solution after etching with NaOH produced brown on A356 coupons; dark brown and black on A380; gold and purple on 6111; and very light gold on 5182 (Fig. 2c). Etching with the $(NH_4)_2MoO_4$ solution after etching with NaOH produced brown and purple on A356 coupons; black on A380; moss-green and purple on 6111; and no change in 5182 (Fig. 2d). Fig. 3 summarizes the two-step etching procedure in a flowchart with the representative colors produced on each alloy coupon. The two-step etching process resulted in distinct colors in each alloy family that can enable rapid optical sorting from each other.

Irrespective of the coloring results, we observed a marked difference in reactions of the different alloy families to the etching solutions. During the initial stages of etching, the coupons bubbled at different rates, indicating a difference in their reactivity. Solutions containing zinc and copper chlorides or sulfates take advantage of this reactivity difference and deposit zinc or copper on the sample surfaces with more reactivity. The only previous study on coloring of aluminum alloy families used copper sulfate solutions (Schultz and Wyss, 2000). When we replicated their study, we also observed a marked difference in copper deposition on coupon surfaces which resulted in red-copper coloring of 6111 and no change in 5182. However, these copper deposits wash off easily with application of water or scraping. The only residue formation that was permanent was produced by the iron chloride solution. Copper residues on sample surfaces can also be costly and further contaminate the scrap stream, and therefore are not recommended. The $KMnO_4$ and $(NH_4)_2MoO_4$ solutions, on the other hand, permanently colored the samples without leaving a residue. These solutions likely formed thin-films oxide layers on the surfaces of the samples (Vander Voort, 2004). The colors are a result of the thin-film interference phenomena, where the coloring in each alloy depends on the thickness of the thin-film layer (Vander Voort, 2004).

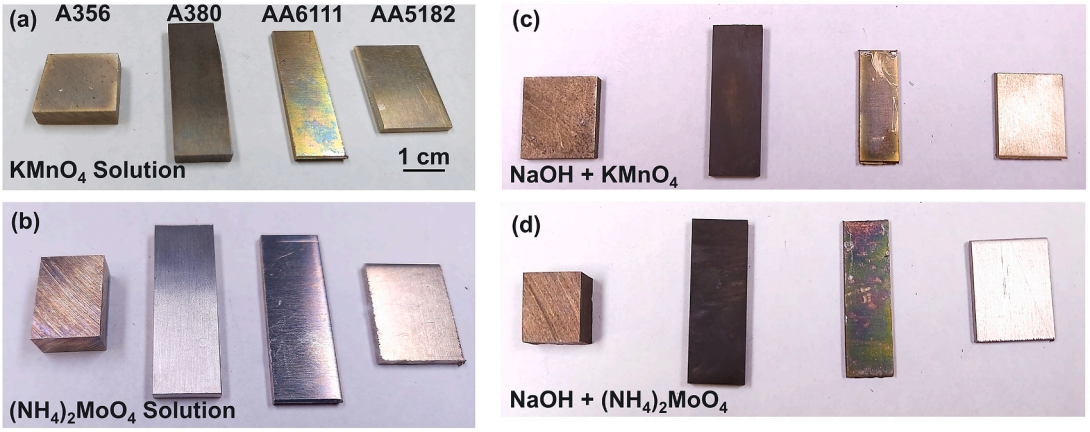

Fig. 2. Photos of the aluminum alloy coupons colored with (a & b) single-step and (c & d) two-step etching process.

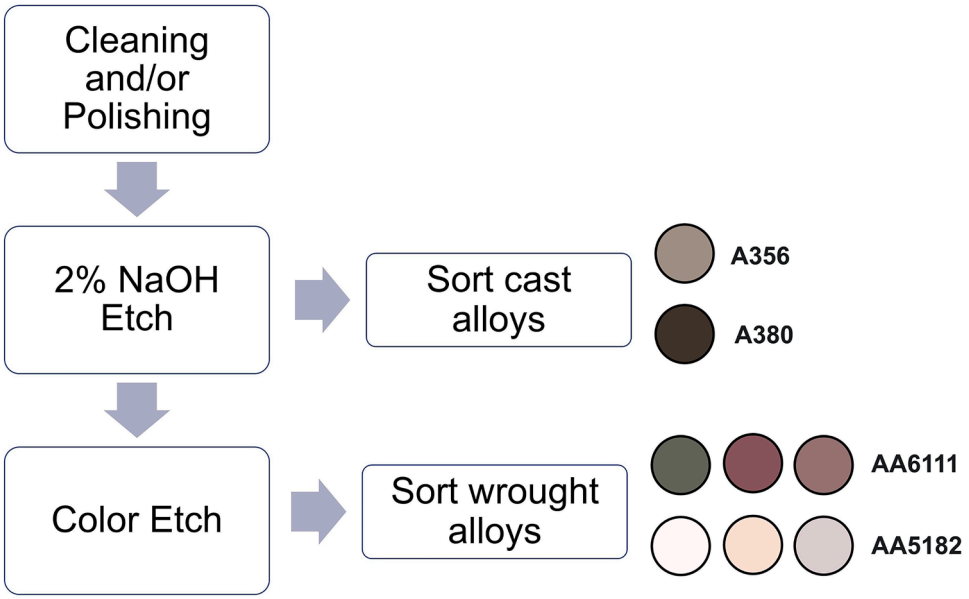

Fig. 3. Flowchart for the proposed coloring and sorting process.

3.2. Color-coding of scrap pieces

After successful etching experiments with the samples of known alloy chemistry, we transitioned to the coloring of actual scrap pieces with unknown alloy chemistry. We hand sorted the mixed Twitch in cast and wrought fractions based on their appearances (Fig. 4a&b). We then etched the pieces by immersing them into NaOH solutions with various concentration and chemistries (Supplementary Table 2). NaOH solutions with concentrations as low as 2 % were able to produce distinct colors within the first two minutes of etching. After etching with NaOH solution, the cast pieces appeared black and wrought pieces appeared a dull, light grey color (Fig. 4c). Due their high alloy content, the cast pieces were significantly more reactive to the etching solution and gradually darkened as etching reactions progressed. Visual examination of the cast pieces confirmed that the black color was a deposited residue likely made from oxides. While this residue was resistant to washing, it was possible to scrape it off by hand. The NaOH solutions also produced distinct colors on uncleaned, as-received scrap pieces, though higher concentrations $>$ 10 % were necessary. Etching at these concentrations provided an additional benefit of removing dirt and contamination from the as-received wrought pieces.

XRF measurements performed on etched pieces confirmed the pieces with black color as cast alloys from the high Si, high Cu family (Fig. 1). The unreacted wrought pieces were confirmed to be 6xxx, 5xxx, 7xxxx and 4xxx alloys. Polishing of some pieces significantly improved XRF accuracy and match quality. Unetched, hand sorted pieces were also correctly identified as cast and wrought alloys by XRF, confirming the hand sorting by appearance. Details of the XRF measurements are

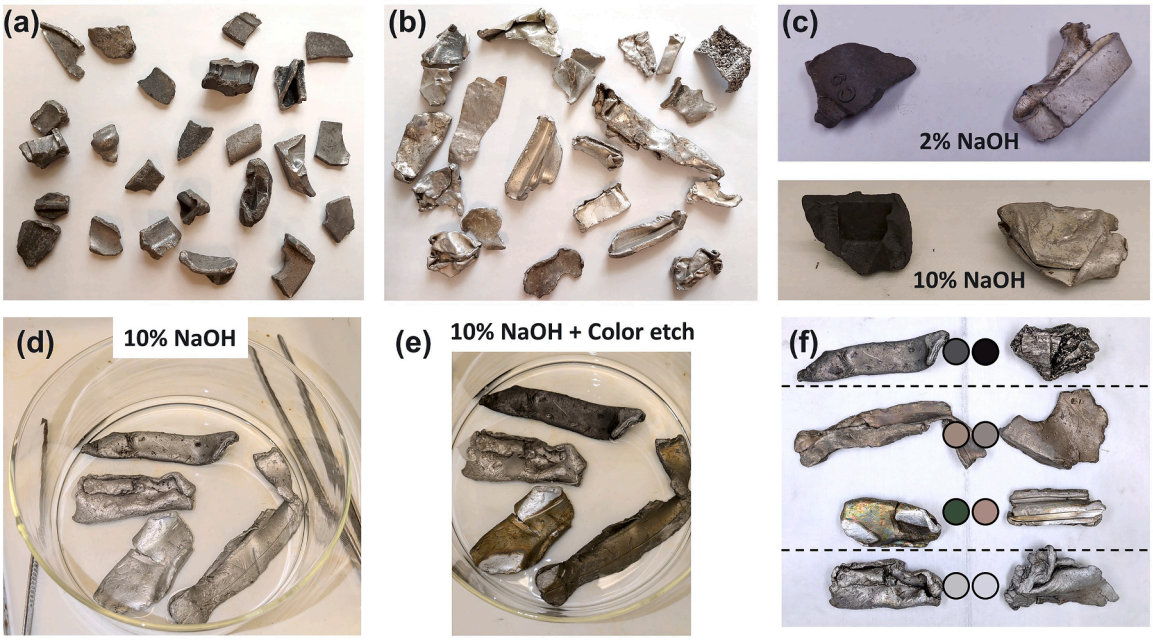

Fig. 4. Photos of the hand sorted (a) cast and (b) wrought scrap pieces. Photos of example cast and wrought scrap pieces after (c) various concentrations of NaOH etching. Photos of wrought scrap pieces (d) after etching in 10 % NaOH for 7 min, (e) during the color etch, and (f) after the color etch.

provided in the supplementary file, along with the photos of the samples used for XRF analysis (Supplementary Fig. 1) and their compositions (Supplementary Table 6).

Wrought scrap pieces were then colored with the two-step procedure to test the feasibility of this procedure on the actual scrap. After etching in a 10 % NaOH solution for 7 min, the wrought scrap pieces had a dull, light grey color (Fig. 4d). The pieces were then etched with the $(NH_4)_2MoO_4$ solution for 12 min. Approximately 6 min were needed to develop the colors shown in Fig. 4e. The annotations in Fig. 4f highlight some of the colors observed in the final pieces. While XRF was not performed on these pieces to confirm their chemistries, the color-coding of known alloy coupons can be used to help identify alloy family. The bottom row of pieces in Fig. 4f are believed to be 5xxx aluminum alloy as they did not develop much color, similar to 5182 in Fig. 2d The pieces in the middle rows of Fig. 4f are believed to by 6xxx aluminum alloy because they developed various brown and green colors, similar to the 6111 alloy in Fig. 2d Finally, the pieces in the top row of Fig. 4f are believed to be 3xxx or 7xxx aluminum alloy. These pieces reacted the most with the color solution, quickly producing dark colors that suggest that these wrought scrap pieces are from alloys with high alloying amounts, such as 3xxx or 7xxx aluminum alloys.

3.3. Optical sorting

Our optical sorter uses a sensitivity profile for certain color-coded materials by "training" it on a number of sample pieces. These sensitivities were created by feeding 5 cast and 5 wrought pieces through the machine during the set-up process where a camera inside the machine took photographs of these training pieces. A sensitivity profile was then generated based on the color of those pieces, which is essentially thresholding RGB color values. The optical sorter measures spectral reflectivity at particular wavelengths, rather than the entire spectrum (Bee and Honeywood, 2004). The sorter then compares the reflectance values of accept and reject materials and there must be a distinctive difference in the values within the selected waveband for a piece to be rejected (Bee and Honeywood, 2004).

In our case, "accepts" were cast pieces in black color and "rejects" were wrought pieces, which were sorted out by means of a pressurized air jet used to shoot individual pieces of the feed material into a different output valve. We also optimized the area parameter to determine an ideal area fraction of the piece that should look like the reject material. Thresholding the color and area is the standard operating principle of the optical sorters used in food sorting (which is also our machine), and it allows users to specify how far from the average product color (in our case black) that the specified area color can deviate before they are rejected (Bee and Honeywood, 2004). After training the machine and setting up the color thresholds and area parameter, we fed a total of 155 mixed cast and wrought pieces through the sorter. It sorted them into two fractions, an "accepted" fraction containing primarily cast pieces and a "rejected" fraction containing primarily wrought pieces. The cast fraction was fed through the machine for a second pass in order to further remove any wrought pieces missed by the first pass.

Fig. 5 shows the scrap pieces optically sorted into cast and wrought fractions. Cast, or accepted fraction, contains mostly uniformly black colored pieces with two uncolored wrought pieces (Fig. 5a). Wrought, or reject fraction, contains mostly uncolored pieces with the exception of four black colored cast pieces (Fig. 5b). Three of these pieces have white paint that might have interfered with the optical sorting (Fig. 5c). These off-color patches are most likely responsible for the optical sorter misidentifying these pieces as wrought, as the color of this paint resembles the color of the wrought pieces used to develop the "reject" profile for this experiment.

Misidentification due to the surface condition, especially paint, dirt or other contamination can be listed as a limitation of the optical sorting method. Our optical sorter requires certain area fraction of color on a piece to pass the “accept” criteria and any variations in color due to paint may have resulted in a reject. Artificial intelligence (AI) assisted computer vision models can be more satisfactory in sorting the color imperfections and paint on the scrap pieces as well as the more varied and colors on the colored wrought scrap pieces (Fig. 4). A well-trained AI model can handle the imperfections in coloring and subtle variations in the appearances at the expense of sorting speeds (Heo et al., 2018; Chen et al., 2021). Recent developments in object detection frameworks such as YOLO (you only look once), integration of various deep learning and machine learning method outputs have improved speed and accuracy AI-based optical sorting operations of metal scrap (Gedam et al., 2025). Combination of latest hardware with faster CNN (convolutional neural networks) architectures have significantly decreased latency to single digits and increased image processing rates in both copper and plastic sorting applications (Koinig et al., 2024; Shukhratov et al., 2024). Implementation of these, and other proposed AI-based computer vision approaches, for accurate sorting of aluminum scrap and at industrial throughput rates remains to be seen. A recent news article reports on the first commercial application of deep learning-based optical sorting of aluminum scrap at 2000 ejections/minute (AI solution upgrades wrought aluminum scrap 2025), equating to ~ 3.1 tons/hr throughput assuming average mass of a scrap piece as 26 g (supplementary file).

Despite the imperfections in the scrap pieces, our optical sorter was successful in achieving high sorting efficiencies as measured by purity of a sorted fraction (Table 1). Purity of each fraction is calculated by:

$$Purity = \frac{True\ Positives}{True\ Positives + False\ Positives}, \quad (1)$$

which resulted in 97 % for the cast fraction, and 95 % for the wrought fraction using the number of pieces. Purity by weight was 97 % for the cast fraction, 93 % for the wrought fraction. Assuming an average of 9.50 wt % Si in cast pieces and 0.45 wt % Si in wrought pieces, the sorted wrought fraction would contain about 1.1 wt % Si if melted. This Si content is within the limits of some 6xxx alloys. A similar case is also

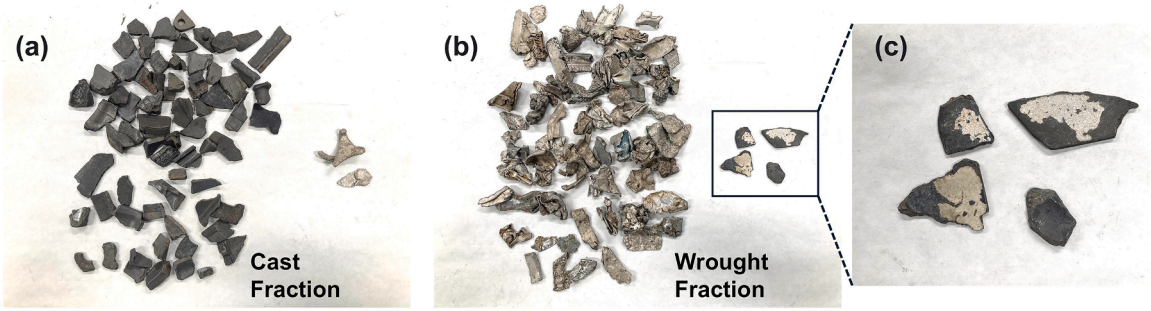

Fig. 5. Photos of the optically sorted (a) cast fraction and (b) wrought fraction. Close-up photo in (c) shows white paint on the cast pieces that were sorted in wrought fraction.

Table 1
Optical sorting results.

	Sorted Cast Fraction				Sorted Wrought Fraction			
	# of pieces	Purity	Weight (g)	Purity	# of pieces	Purity	Weight (g)	Purity
Cast Pieces	70	97 %	401.25	97 %	4	5 %	15.69	7 %
Wrought Pieces	2	3 %	12.17	3 %	79	95 %	200.67	93 %
Total	72	100 %	413.42	100 %	83	100 %	216.36	100 %

true for Fe and Cu contents, and it is possible to obtain a secondary 6xxx alloy by melting the sorted wrought scrap (Das et al., 2007). One concern could be the alloying elements coming from other wrought alloys, such the high Mg 5xxx, high Zn 7xxx, or high Si 4xxx. However, as shown in Fig. 3, the coloring chemicals used in this study can develop colors in the individual wrought alloy families to reduce contamination from the high alloy content wrought alloys.

3.4. Economic feasibility, environmental concerns, and implications for the U.S. aluminum and transportation industries

We envision the color sorting process to work in the conceptual line shown in the graphical abstract. The coloring process can be integrated after the pre-sorting steps such as floatation and the coloring chemicals can be sprayed on the scrap pieces traveling on a conveyor belt. While we showcased spraying for coloring and air knives for the ejection steps in the graphical abstract for simplicity, immersion in chemical baths and ejection by air jets can be alternatives to the spraying and air knife ejection steps, respectively. Some potential benefits of using an immersion bath include more thoroughly coloring the pieces (as using a sprayer risks only the top surface of the pieces etching) and less evaporation of the chemical solution. However, an immersion bath would also require more chemicals and would require equipment that is more thoroughly protected against corrosion, which could increase material costs. We assumed immersion bath method for our TEA. For the coloring step, chemical reactions can be accelerated by external stimulants like heat and agitation to keep up with the scrap pieces moving at speeds of 0.5–2 m/s at commercial operations. The chemicals used in our process are considered practically non-toxic and not an irritant (Category 4) or slightly toxic and slightly irritating (Category 3), per their Safety Data Sheets according to Globally Harmonized System of Classification. While being mildly or non-toxic, some of these chemicals are corrosive and can be hazardous to aquatic life. However, they are used in low-concentration (< 5 %) water solutions. The aluminum industry is experienced in designing equipment to address corrosion issues and in neutralizing and disposing of chemical waste. In this study, it is assumed that all equipment in contact with NaOH is made of 316 stainless steel due to corrosion concerns. Additionally, NaOH will be neutralized with acetic acid for safe disposal. The neutralization reaction produces byproducts that are environmentally benign and does not generate excessive amounts of heat.

To evaluate the economic viability and environmental friendliness of our process, we conducted techno-economic analysis and life cycle analysis. The current price cap between Twitch and primary aluminum is ~44 ¢/kg in the U.S. (Petras, 2023). We estimate our process will add ~4.48 ¢/kg to the cost, with 0.13 ¢/kg for materials, 0.46 ¢/kg for utilities, 0.97 ¢/kg for labor, 1.28 ¢/kg for capital, and 1.64 ¢/kg for other expenses. This cost includes the neutralization of the chemicals for safe disposal. Even when the etching solution cannot be reused, the cost is only 9.27 ¢/kg (with additional 4.17 ¢/kg for chemicals). This could translate into significant operating margins considering the sheer quantity of scrap generated in the U.S. (3.6 million metric tons) (Merrill, 2025).

Moreover, as Table 1 shows, our color sorting method can separate mixed aluminum scrap into relatively pure wrought and cast streams. Having a pure wrought aluminum stream for recycling can transform the aluminum supply chain and its environmental impacts, particularly for the transportation industry as it is the largest consumer of aluminum in the U.S. (Merrill, 2025). The wrought aluminum content in North American light-duty vehicles is expected to further increase from 73 kg per vehicle in 2020 to 115 kg in 2030, while the cast aluminum content would only increase from 136 to 138 kg (2023 North American Light Vehicle Aluminum Content and Outlook 2023). This poses two problems. First, the amount of available aluminum scrap may outgrow the demand for cast aluminum and result in an excess supply of scrap that is not recycled (Zhu et al., 2021). Second, with 15.25 million light vehicles sales projected for the U.S. in 2030 (Annual Energy Outlook 2023), 1.75 million metric ton (MMT) of wrought aluminum will be required for the automotive industry alone, while the U.S. only produced 0.67 MMT of primary aluminum in 2024 (Merrill, 2025).

By enabling closed-loop wrought-to-wrought aluminum recycling, our sorting technology thus paves the way to use alternative domestic aluminum resources to manufacture high-performance, lower embodied energy components for applications such as automative closure sheets, structural members (body-in-white), battery trays of electric vehicles, solar panels, electric transmission wires, extrusions for buildings, and consumer durables. U.S. imports ~ 3.8 MMT of aluminum per year for its consumption, while exporting 2.1 MMT of scrap (Merrill and Weaver, 2024). With the increased in recycled content from 25 % to 80 %, it is possible to replace ~ 1.5 MMT of imported primary aluminum with the 2.1 MMT of domestic scrap resources that are currently exported to be mainly downcycled into low performance, non-structural products. Additionally, utilization of domestic scrap resources has the potential to significantly reduce the energy dependency of the aluminum industry. Compared with virgin aluminum, secondary aluminum is 88 % lower in embodied energy, and 89 % lower in carbon intensity (R&D GREET® Model 2025). Our life cycle analysis finds that the total energy consumption of our process is 0.70 MJ/kg Twitch sorted, and the carbon footprint is 0.04 kgCO_2e/kg. If our technology makes it possible to meet the 1.75 MMT wrought aluminum demand through recycling, 186.73 PJ of energy can be saved, and 12.2 MMT of CO_2 emissions can be avoided.

4. Summary

We demonstrated rapid, low-cost optical sorting of cast and wrought aluminum pieces from the post-consumer Twitch scrap stream. To enable the optical sorting, we developed a color-coding process by reacting the scrap pieces with non-acidic chemicals. Reaction with sodium hydroxide (NaOH) solutions with concentrations as low as 2 % was enough to change color of the actual cast scrap pieces. The colored cast scrap pieces were then optically sorted from the wrought scrap with purities > 95 %. We also showed a two-step coloring process which resulted in distinct colors in coupons of two cast alloys, A356 and A380, and two wrought alloys, 6111 and 5182, and wrought scrap that are commonly found in the Twitch stream. The two-step process can enable optical sorting of cast from wrought as well as sorting of wrought scrap into individual alloy families. Chemical analysis of the sorted wrought scrap showed compositions conforming to 6xxx alloys if melted, which suggests that low-cost optical sorting can enable manufacturing of wrought products made from high recycle content 6xxx alloys.

Our TEA and LCA showed economic feasibility of the process with the added benefit of making sorted wrought scrap abundant, which paves the way to use alternative domestic aluminum resources to manufacture high-performance, lower embodied energy components for

applications such as transportation, electrical, and consumer durables. The increase in recycled content of high performance wrought and cast aluminum products has the potential to replace ~ 1.5 MMT of imported primary aluminum in U.S. with the domestic scrap resources, while significantly reducing the energy consumption of the aluminum industry.

CRediT authorship contribution statement

Mert Efe: Writing – review & editing, Writing – original draft, Visualization, Validation, Project administration, Methodology, Investigation, Funding acquisition, Formal analysis, Data curation, Conceptualization. **Aashish Rohatgi:** Writing – review & editing, Writing – original draft, Methodology, Formal analysis. **Qiang Dai:** Writing – review & editing, Writing – original draft, Validation, Software, Methodology, Formal analysis, Data curation. **Brian Stapleton:** Writing – review & editing, Writing – original draft, Visualization, Validation, Resources, Methodology, Investigation, Formal analysis, Data curation. **Kate Rader:** Writing – review & editing, Visualization, Validation, Methodology, Formal analysis, Data curation. **Albert L. Lipson:** Writing – review & editing, Validation, Resources, Methodology, Investigation, Data curation. **Jeffrey S. Spangenberger:** Writing – review & editing, Software, Resources, Methodology, Funding acquisition, Conceptualization.

Declaration of competing interest

The authors declare the following financial interests/personal relationships which may be considered as potential competing interests:

Mert Efe reports financial support was provided by U.S. Department of Energy, Office of Energy Efficiency and Renewable Energy, Vehicle Technologies Office. If there are other authors, they declare that they have no known competing financial interests or personal relationships that could have appeared to influence the work reported in this paper.

Acknowledgements

Funding for this work was provided by the U.S. Department of Energy, Office of Energy Efficiency and Renewable Energy, Vehicle Technologies Office, through the LightMAT and Lightweight Metals Core Programs (LMCP). We appreciate the support and technical guidance by Darrell Herling, Tim Skszek, and Glenn Grant. We thank Anthony Guzman and Gabrielle Schuler for their help with the etching experiments, and Shivakant Shukla and Landon Walker for their help with the XRF measurements. The Pacific Northwest National Laboratory (PNNL) is operated by the Battelle Memorial Institute for the Department of Energy under contract DE-AC05–76RL01830. Optical sorting was conducted at the Materials Engineering Research Facility, Argonne National Laboratory, a U. S. Department of Energy Office of Science laboratory operated by UChicago Argonne, LLC under contract DE-AC02–06CH11357.

Supplementary materials

Supplementary material associated with this article can be found, in the online version, at doi:10.1016/j.resconrec.2025.108500.

Data availability

Data will be made available on request.

References

AI solution upgrades wrought aluminum scrap, 2025. https://www.recyclingproductnews.com/article/43077/ai-solution-upgrades-wrought-aluminum-scrap. Accessed 28/05/2025.

Ambrose, F., Brown, R.D., Montagna, D., Makar, H.V., 1983. Hot-crush technique for separation of cast- and wrought-aluminum alloy scrap. Conserv. Recycl. 6 (1), 63–69.

Annual Energy Outlook 2023, U.S. Energy Information Administration, https://www.eia.gov/outlooks/aeo/, 2023.

Bee, S.C., Honeywood, M.J., 2004. Optical sorting systems. In: Edwards, M. (Ed.), Detecting Foreign Bodies in Food. CRC Press, FL, pp. 86–118.

Beraha, E., Shpigler, B., 1977. Color metallography. Am. Soc. Metals.

Brooks, L., Gaustad, G., 2021. The potential for XRF & LIBS handheld analyzers to perform material characterization in scrap yards. J. Sustain. Metall. 7 (2), 732–754.

Chen, S., Hu, Z., Wang, C., Pang, Q., Hua, L., 2021. Research on the process of small sample non-ferrous metal recognition and separation based on deep learning. Waste Manag. 126, 266–273.

Das, S.K., Green, J.A.S., Kaufman, J.G., 2007. The development of recycle-friendly automotive aluminum alloys. JOM 59 (11), 47–51.

Das, S.K., Green, J.A.S., Kaufman, J.G., Emadi, D., Mahfoud, M., 2010. Aluminum recycling—An integrated, industrywide approach. JOM 62 (2), 23–26.

Díaz-Romero, D., Sterkens, W., Van den Eynde, S., Goedemé, T., Dewulf, W., Peeters, J., 2021. Deep learning computer vision for the separation of cast- and wrought-aluminum scrap. Res., Conserv. Recycl. 172, 105685.

Gedam, P.B., Khan, A., Purohit, N., Jha, V.K., 2025. A systematic review: development of AI based computer vision scrap sorting system for metal scrap. In: 2025 International Conference on Multi-Agent Systems for Collaborative Intelligence (ICMSCI), pp. 876–881.

Gülcan, E., Gülsoy, Ö.Y., 2017. Performance evaluation of optical sorting in mineral processing – A case study with quartz, magnesite, hematite, lignite, copper and gold ores. Int. J. Miner. Process. 169, 129–141.

Heo, Y.J., Kim, S.J., Kim, D., Lee, K., Chung, W.K., 2018. Super-high-purity seed sorter using low-latency image-recognition based on Deep learning. IEEE Robot. Autom. Lett. 3 (4), 3035–3042.

Kelly, S., Apelian, D., 2017. Value creation through enabling technologies to up-cycle aluminum scrap. In: ESS: M&R3 SME Symposium. Denver, CO.

Koinig, G., Kuhn, N., Fink, T., Lorber, B., Radmann, Y., Martinelli, W., Tischberger-Aldrian, A., 2024. Deep learning approaches for classification of copper-containing metal scrap in recycling processes. Waste Manag. 190, 520–530.

Koyanaka, S., Kobayashi, K., 2010. Automatic sorting of lightweight metal scrap by sensing apparent density and three-dimensional shape. Res., Conserv. Recycl. 54 (9), 571–578.

Løvik, A.N., Modaresi, R., Müller, D.B., 2014. Long-term strategies for increased recycling of automotive aluminum and its alloying elements. Environ. Sci. Technol. 48 (8), 4257–4265.

Merrill, A., Weaver, S., 2024. Aluminum in December 2023, Mineral Industry Surveys. U. S. Geological Survey. https://www.usgs.gov/centers/national-minerals-information-center/aluminum-statistics-and-information.

Merrill, A., 2025. Aluminum, Mineral Commodity Summaries. U.S. Geological Survey. https://www.usgs.gov/centers/national-minerals-information-center/aluminum-statistics-and-information.

Newman, L., 2018. Etching of Aluminum and Its Alloys. In: Anderson, K., Weritz, J., Kaufman, J.G. (Eds.), *Aluminum Science and Technology*. ASM International, pp. 586–589.

2023 North American Light Vehicle Aluminum Content and Outlook, Ducker Research and Consulting/DUCKER HOLDINGS LLC, https://drivealuminum.org/resources-post/2023-north-american-light-vehicle-aluminum-content-and-outlook/, 2023.

K. Petras, US aluminium scrap, secondary alloy prices mixed on quieter market, 2023. https://www.fastmarkets.com/insights/us-aluminium-scrap-secondary-alloy-prices-mixed-quieter-market/. Accessed 31/03/2025.

R&D GREET® Model, 2025. https://greet.anl.gov/. Accessed 31/03/2025.

Raabe, D., Ponge, D., Uggowitzer, P.J., Roscher, M., Paolantonio, M., Liu, C., Antrekowitsch, H., Kozeschnik, E., Seidmann, D., Gault, B., De Geuser, F., Deschamps, A., Hutchinson, C., Liu, C., Li, Z., Prangnell, P., Robson, J., Shanthraj, P., Vakili, S., Sinclair, C., Bourgeois, L., Pogatscher, S., 2022. Making sustainable aluminum by recycling scrap: the science of "dirty" alloys. Prog. Mater. Sci. 128, 100947.

Schlesinger, M.E., 2013. Aluminum Recycling, 2nd ed. CRC Press.

Schultz, P., Wyss, R., 2000a. Color sorting aluminum alloys for recycling. Part I, Plat. Surface Finish. 87 (4), 10–12.

Schultz, P., Wyss, R., 2000b. Color sorting aluminum alloys for recycling-part II. Plat. Surface Finish. 87 (6), 62–65.

Shukhratov, I., Pimenov, A., Stepanov, A., Mikhailova, N., Baldycheva, A., Somov, A., 2024. Optical detection of plastic waste through computer vision. Intelligent Syst. Applic. 22, 200341.

Tansens, P., Rodal, A.T., Machado, C.M.M., Soares, H.M.V.M., 2011. Recycling of aluminum and caustic soda solution from waste effluents generated during the cleaning of the extruder matrixes of the aluminum industry. J. Hazard. Mater. 187 (1), 459–465.

Van den Eynde, S., Bracquené, E., Diaz-Romero, D., Zaplana, I., Engelen, B., Duflou, J.R., Peeters, J.R., 2022. Forecasting global aluminium flows to demonstrate the need for improved sorting and recycling methods. Waste Manag. 137, 231–240.

Vander Voort, G.F., 1999. Metallography, Principles and Practice. ASM International.

Vander Voort, G.F., 2004. Color metallography. In: Vander Voort, G.F. (Ed.), Metallography and Microstructures. ASM International, pp. 493–512.

Warmuzek, M., 2004. Metallographic techniques for aluminum and its alloys. In: Vander Voort, G.F. (Ed.), Metallography and Microstructures. ASM International, pp. 711–751.

Weck, E., Leistner, E., 1983. Metallographic Instructions for Colour Etching By Immersion. Deutscher Verlag fur Schweisstechnik.

Williams, K.C., Mallaburn, M.J., Gagola, M., O'Toole, M.D., Jones, R., Peyton, A.J., 2023. Classification of shredded aluminium scrap metal using magnetic induction spectroscopy. Sensors 23 (18), 7837.
Zhu, Y., Chappuis, L.B., De Kleine, R., Kim, H.C., Wallington, T.J., Luckey, G., Cooper, D. R., 2021. The coming wave of aluminum sheet scrap from vehicle recycling in the United States. Res., Conservat. Recycl. 164, 105208.
Zhu, Y., Khan, O., Heidari, M., Tsai, A., Chappuis, L., Chiriac, C., Freiberg, D., Hamid, A., Kim, H.C., De Kleine, R., Sundararajan, A., Cooper, D.R., 2025. Analysis of scrap flows from recycling aluminum-intensive vehicles in the United States: insights from a case study on the F-150. Res., Conserv. Recycl. 217, 108199.